2.482 Å (total range 2.430 (9)-2.498 (5) Å) for $[W_2S_4(S_2P(OEt)_2)_2]$. In lower valent $[W_4S_4(S_2P(OEt)_2)_6]$, W-S(dithiophosphate) bond lengths average 2.548 Å (range 2.542 (6)-2.560 (6) Å) for the bidentate ligand.[16]

Discussion

$[W(NTo)(S_2P(OEt)_2)S]_4$ has shown modest differences from $[Mo(NTo)(S_2P(OEt)_2)S]_4$, although the associative equilibrium of eq 1 is notably less favored for the former. Spectroscopic evidence (IR and NMR) suggests differences in σ and π interactions with the organic coligands, although a fuller evaluation of these would require examination of more derivatives. Structurally the two compounds are very similar, as demonstrated by the comparison in Table V. There are only two differences suggested by that comparison: W-W bonds are longer than Mo-Mo bonds, and the long M-S bonds are perhaps longer for W than for Mo. Interestingly, direct W vs Mo comparisons of structural results for analogous *syn*-$M_2(\mu\text{-}S)_2$ complexes of the pentavalent metals have previously revealed few differences, even in M-M bond lengths.[43,45-47,50]

Comparisons between pentavalent $[W(NTo)(S_2P(OEt)_2)S]_4$ and mixed-valent (III/IV) $[W_4S_4(S_2P(OEt)_2)_6]$ are somewhat limited, due in part to their different symmetries. The latter is distorted trigonally from a cube and can be idealized to C_{3v} symmetry, giving a $W_3W'S_3S'$ arrangement.[55] The elongation in $[W(NTo)(S_2P(OEt)_2)S]_4$ gives idealized D_{2d} symmetry and retains equivalence of all metal positions. The two compounds also differ substantially in cluster metal electron count,[24] giving different numbers of W-W bonds.

The mixed-metal cluster $[W_2Mo_2(NTo)_4(S_2P(OEt)_2)_4S_4]$, observed in solution, represents an example of a W/Mo cuboidal complex constructed from dimer fragments. Two forms of a mixed-metal, Mo_3WS_4, compound, $[Mo_3WS_4(S_2PEt_2)_6]$, have been reported; these were obtained from the reaction of a Mo_3 trimer and a W monomer.[30] The use of two different metal dimers and the use of the trimer/monomer combination have proven useful for other mixed-metal cuboidal complexes.[25,30,31,56] One form of $[Mo_3WS_4(S_2PEt_2)_6]$ was also crystallographically characterized, and the structure is, in fact, analogous (except for the phosphinate/phosphate difference) to the above-cited W_4S_4 derivative, $[W_4S_4(S_2P(OEt)_2)_6]$.

Use of $[W(NTo)(S_2P(OEt)_2)S]_4$ for generating sulfur-reactive dimers of the type $[W_2(NTo)_2(S_2P(OEt)_2)_2(\mu\text{-}S)_2(\mu\text{-}O_2CR)]^-$ has been undertaken. Interestingly, despite the similarities in the cuboidal W_4S_4 and Mo_4S_4 precursors, notable differences have been realized between the sulfur-based chemistries of the W_2S_2 and Mo_2S_2 dimers, particularly in the chemistries of $M_2(\mu\text{-}SH)$ types.[15] This work is in progress.

Acknowledgment. This work was supported by a research award from the National Science Foundation.

Supplementary Material Available: Tables of full crystallographic parameters, positional parameters of all atoms, general displacement parameters, bond lengths, bond angles, and least-squares WS_2 planes (19 pages); a table of structure factors (28 pages). Ordering information is given on any current masthead page.

(55) Preliminary information on a D_{2d} form of $[W_4S_4(S_2P(OEt)_2)_6]$ was communicated in ref 17.

(56) Zhi-da, C.; Jia-xi, L.; Chun-wan, L.; Qian-er, Z. *J. Mol. Struct.* **1991**, *236*, 343.

Contribution from the Department of Chemistry, University of California, Davis, California 95616

Reactivity of Complexes with Weak Metal-Metal Bonds. Reactions of Lewis Acids with $[AuIr(CO)Cl(\mu\text{-}Ph_2PCH_2PPh_2)_2](PF_6)$

Alan L. Balch* and Vincent J. Catalano

Received November 21, 1991

The dinuclear complex $[AuIr(CO)Cl(\mu\text{-dpm})_2](PF_6)$ (**1**; dpm is bis(diphenylphosphino)methane) is unreactive in dichloromethane solution toward substances (trifluoroacetic acid, hydrogen chloride, sulfur dioxide, dihydrogen, tetracyanoethylene) that are known to bind to $Ir(CO)Cl(PPh_3)_2$. A weak adduct is formed with boron trifluoride. Both **1** and $[AuIr(CNMe)_2(\mu\text{-dpm})_2](PF_6)_2$ react with mercury(II) chloride in a two-step process. At low temperature an unstable intermediate with the $Au(\mu\text{-dpm})_2Ir$ core intact is formed. This is formulated as an A-frame with a $HgCl_2$ moiety bonded to the AuIr unit. On warming, one of the bridging dpm units opens and $Cl_2Hg(\mu\text{-}Cl)_2HgIr(CO)Cl(dpm)(\mu\text{-dpmAuCl})$ is formed. Ivory parallelepipeds of this form in the monoclinic space group $P2_1/c$ with a = 10.594 (7) Å, b = 25.12 (2) Å, c = 21.397 (13) Å, β = 91.04 (5)° at 130 K with Z = 4. Refinement of 3974 reflections and 365 parameters yielded R = 0.067 and R_w = 0.061. The structure contains four metal centers each with a different coordination number, 2 for gold, 3 and 4 for mercury, and 6 for iridium.

Introduction

The nature of the metal-metal bonding in dinuclear d^8-d^8 and d^{10}-d^{10} dimers has led to considerable understanding of their characteristic electronic absorption and emission spectra.[1-4] Some aspects of their chemical reactivity have been probed, particularly the photoinduced oxidative addition chemistry of $[Pt_2(P_2O_5H_2)_4]^{4-}$. We have recently explored the structural and spectroscopic features of heterodinuclear species involving one d^{10} metal center and one d^8 metal center.[5,6] One of these, $[AuIr(CO)Cl(\mu\text{-dpm})_2](PF_6)$ (**1**; dpm is bis(diphenylphosphino)methane), contains a planar

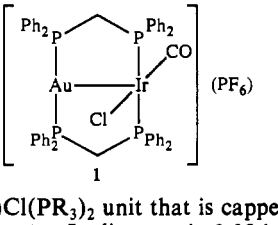

1

Vaska-type $Ir(CO)Cl(PR_3)_2$ unit that is capped by a linear P-Au-P portion. The Au-Ir distance is 2.986 (1) Å.[5] This is significantly longer than simple Ir-Au single bonds where the corresponding distances fall in the 2.59-2.81-Å range.[6-10]

(1) Roundhill, D. M.; Gray, H. B.; Che, C.-M. *Acc. Chem. Res.* **1989**, *22*, 55.
(2) Zipp, A. P. *Coord. Chem. Rev.* **1988**, *84*, 47.
(3) Khan, M. N. I.; Fackler, J. P., Jr.; King, C.; Wang, J. C.; Wang, S. *Inorg. Chem.* **1988**, *27*, 1672.
(4) Che, C.-M.; Wong, W. T.; Lai, T.-F.; Dwong, H.-L. *J. Chem. Soc., Chem. Commun.* **1989**, 243.
(5) Balch, A. L.; Catalano, V. J.; Olmstead, M. M. *Inorg. Chem.* **1990**, *29*, 585.
(6) Balch, A. L.; Catalano, V. J. *Inorg. Chem.* **1991**, *30*, 1302.
(7) Casalnuovo, A. L.; Pignolet, L. H.; van der Velden, J. W. A.; Bour, J. J.; Steggerda, J. J. *J. Am. Chem. Soc.* **1983**, *105*, 5957.
(8) Casalnuovo, A. L.; Laska, T.; Nilsson, P. V.; Olofson, F.; Pignolet, L. H. *Inorg. Chem.* **1985**, *24*, 233.
(9) Casalnuovo, A. L.; Casalnuovo, J. A.; Nilsson, P. V.; Pignolet, L. H. *Inorg. Chem.* **1985**, *24*, 2554.
(10) Casalnuovo, A. L.; Laska, T.; Nilsson, P. V.; Olofson, J.; Pignolet, L. H.; Bos, W.; Bour, J. J.; Steggerda, J. J. *Inorg. Chem.* **1985**, *24*, 182.

0020-1669/92/1331-2730$03.00/0

However, such a distance is comparable to those found in d^{10}–d^{10} and d^8–d^8 dimers where the metal–metal interaction has a significant effect on physical properties of the individual components and on their chemical reactivity as well.[1,2] We have recently shown that addition of a Lewis base to a related IrAu dinuclear complex, **2**, results in the *strengthening and shortening* of the metal–metal bond (eq 1).[6] This was attributed to the formation of a dative Ir→Au bond in the product **3**.

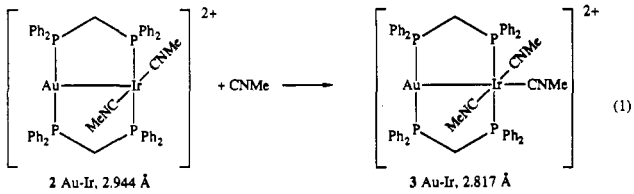

(1)

Here we investigate the reactivity of **1** and **2** toward Lewis acids. The mononuclear prototype, $Ir(CO)Cl(PPh_3)_2$, is well-known to display Lewis basicity and under goes addition reactions with a wide variety of substances[14] (e.g. H_2, O_2, tetracyanoethylene, C_{60},[15] and C_{70}[16]). Here the effect of the proximity of the gold center on the reactivity of the iridium ion is examined.

Results and Discussion

Reactivity of 1 and 2 with Lewis Acids. The Au/Ir complexes **1** and **2** are considerably less reactive than $Ir(CO)Cl(PPh_3)_2$ toward addition of Lewis acids.[14] Both **1** and **2** can be handled in solutions exposed to the atmosphere. These show no decomposition for many hours and no evidence for the formation of a dioxygen adduct. Treatment of solutions of **1** with an excess of trifluoroacetic acid, hydrogen chloride, sulfur dioxide, dihydrogen, or tetracyanoethylene results in no alteration of the characteristic electronic absorption spectrum of **1**. From these observations, we conclude that the proximity of the gold ion to the $Ir(CO)Cl(P)_2$ unit considerably reduces the reactivity of the iridium ion. The lack of reactivity toward sulfur dioxide is particularly interesting since the trinuclear complex $[Ir_2(CO)_2Cl_2Au\{\mu\text{-}(Ph_2PCH_2)_2AsPh\}_2](PF_6)$ does add sulfur dioxide to one of the square $Ir(CO)ClP_2$ faces.[17]

However, **1** is reactive toward both boron trifluoride and mercury(II) chloride. Addition of boron trifluoride or boron trifluoride etherate to an orange solution of **1** results in a color change to yellow. The $^{31}P\{^1H\}$ NMR spectrum of the resulting solution shows a clean set of two, five-line patterns at 10.0 and 38.0 ppm which are consistent with an AA′XX′ spin system. Attempts to isolate the adduct have been frustrated by its ready reversion to **1**. Thus, addition of alcohols, ethers, ketones, or chlorinated hydrocarbons to solutions of the boron trifluoride adduct resulted in its conversion back to **1**. In an attempt to ascertain whether the boron trifluoride was bonding to a metal (probably iridium) or to the chloride ligand in **1**, the reaction between boron trifluoride and **2** was examined. In the presence of boron trifluoride, **2** turns colorless, and the $^{31}P\{^1H\}$ NMR spectrum shows that a variety of products are formed. Because of the difference of reactivity in **1** and **2**, we conclude that the adduct formed from **1** and BF_3 probably involves the formation of a boron–chlorine bond.

Addition of mercury(II) chloride to **1** and **2** occurs in two steps that can be readily observed by carrying the reaction out at low temperature and then allowing the sample to warm. Trace A of Figure 1 shows the $^{31}P\{^1H\}$ NMR spectrum of **1** in dichloromethane solution. Trace B shows the spectrum after the addition of an excess of mercury(II) chloride at −70 °C. The resonances of **1** have been replaced by new resonances of an intermediate **4**. These resonances appear as a pair of apparent triplets. Each resonance is flanked by satellites due to coupling to ^{199}Hg (17% natural abundance, spin = $^1/_2$). The Hg–P coupling for the low-field resonance is 565 Hz, while for the upfield resonance it is 244 Hz. On warming, the resonances of **4** undergo some broadening, and a set of new resonances appear. These are readily seen in trace C, which was obtained by warming the sample to −10 °C. Further warming results in further conversion of **4** into the new species **5**. Complex **5**, $Cl_2Hg(\mu\text{-}Cl)_2HgIr(CO)Cl\text{-}(dpm)(\mu\text{-}dpmAuCl)$, can be isolated as ivory crystals from the reaction between **1** and mercury(II) chloride at 25 °C. It has been crystallized and thoroughly characterized by X-ray crystallography (vide infra). The $^{31}P\{^1H\}$ NMR spectrum obtained from **5** is shown in Figure 2. This spectrum is readily explained by the structure of this tetranuclear complex. The resonance A at low field is due to the phosphorus atom of the P–Au–Cl unit. The high-field signal D with large satellites due to coupling to

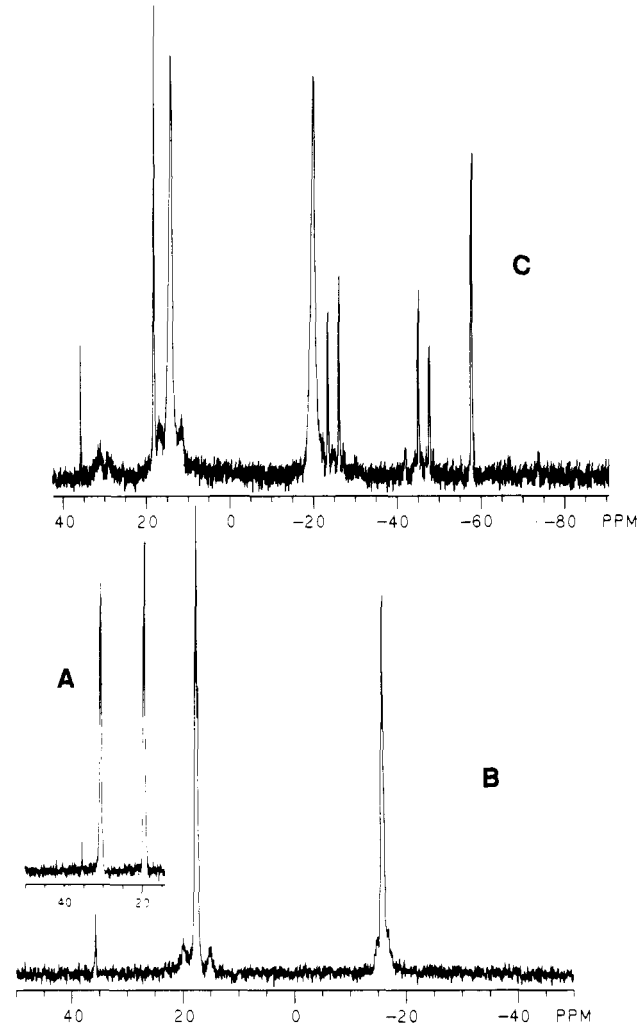

Figure 1. $^{31}P\{^1H\}$ NMR spectra of (A) $[AuIr(CO)Cl(\mu\text{-dpm})_2](PF_6)$ (**1**), (B) **1** after the addition of $HgCl_2$ at −70 °C, and (C) the same sample after warming to −10 °C. The solvent is dichloromethane.

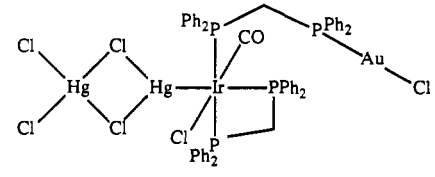

5

(11) Luke, M. A.; Mingos, D. M. P.; Sherman, K. J.; Wardle, R. W. M. *Transition Met. Chem.* **1987**, *12*, 37.
(12) Balch, A. L.; Nagle, J. K.; Oram, D. E.; Reedy, P. E., Jr. *J. Am. Chem. Soc.* **1988**, *110*, 454.
(13) Balch, A. L.; Catalano, V. J.; Olmstead, M. M. *J. Am. Chem. Soc.* **1990**, *112*, 2010.
(14) Vaska, L. *Acc. Chem. Res.* **1968**, *1*, 335.
(15) Balch, A. L.; Catalano, V. J.; Lee, J. W. *Inorg. Chem.* **1991**, *30*, 3980.
(16) Balch, A. L.; Catalano, V. J.; Lee, J. W.; Olmstead, M. M.; Parkin, S. P. *J. Am. Chem. Soc.* **1991**, *113*, 8953.
(17) Balch, A. L.; Davis, B. J.; Olmstead, M. M. *Inorg. Chem.* **1989**, *28*, 3148.

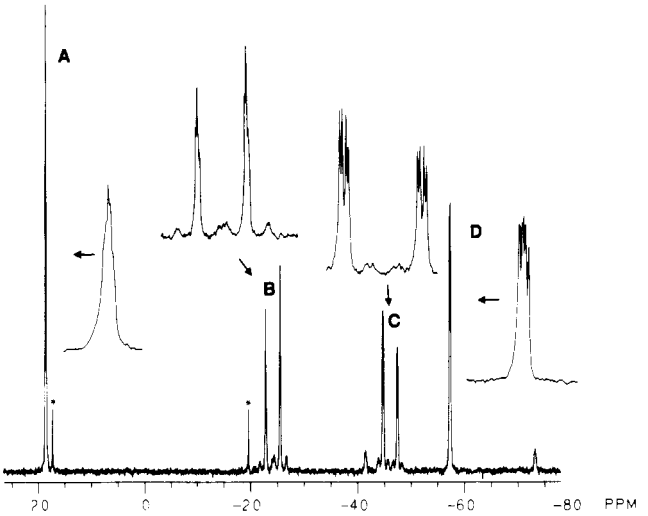

Figure 2. $^{31}P\{^1H\}$ NMR spectrum of $Cl_2Hg(\mu\text{-}Cl)_2HgIr(CO)Cl(dpm)(\mu\text{-}dpmAuCl)$ (**5**) in dichloromethane. The two peaks labeled with asterisks arise from unidentified impurities.

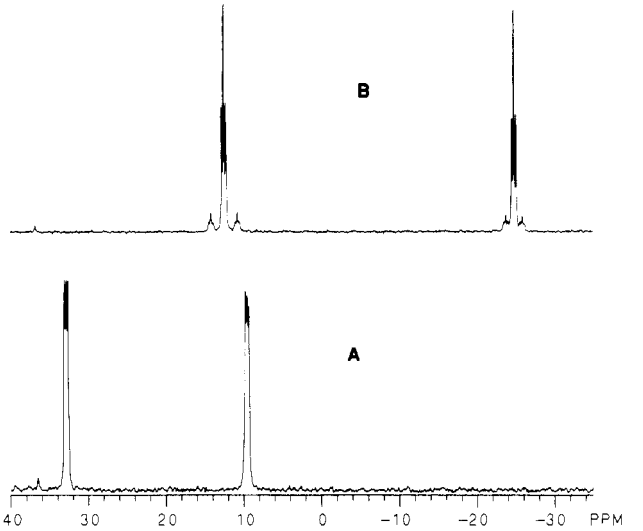

Figure 3. $^{31}P\{^1H\}$ NMR spectra of $[AuIr(CNCH_3)_2(\mu\text{-}dpm)_2](PF_6)$ (**2**) in acetone: (A) **2** alone; (B) sample after the addition of $HgCl_2$ at −50 °C.

mercury comes from the phosphorus atom trans to the mercury ligand. The Hg–P coupling constant (3822 Hz) is consistent with the presence of a *trans*-Hg–Ir–P unit.[18] The AB doublet pattern, which consists of resonances B and C, is assigned to the pair of trans phosphorus atoms that are bound to iridium. The P–P coupling constant of 325 Hz is reasonable for such a trans arrangement.[19] Each of the resonances in B and C shows satellites due to coupling to mercury. The coupling constants in both cases are 225 Hz. These are consistent with the presence of *cis*-Hg–Ir–P units.[18] The infrared spectrum of the isolated product shows a band at 2060 cm^{-1} that is assigned to the terminal carbon monoxide. This is 103 cm^{-1} higher than that of **1** (1957 cm^{-1}). Thus, there is significant removal of electron density from iridium in the formation of **5**.[14]

Mercury(II) chloride also reacts with **2** to form an intermediate that is similar to **4**. Relevant $^{31}P\{^1H\}$ NMR spectra are shown in Figure 3. Trace A shows the spectrum of **2** alone. Addition of mercury(II) chloride at ~50 °C converts that spectrum into the one shown in trace B. The features of **2** have been lost and a new set of resonances, attributed to an intermediate **6** are present. Two equally intense apparent triplets are present, each flanked by satellites due to coupling to mercury. The Hg–P coupling for the low-field resonances (417 Hz) is larger than that for the upfield resonance (292 Hz). On warming, the resonances due to **6** are replaced by a set of four resonances that are similar but not identical to those seen in Figure 2.

The structure of the intermediates **4** and **6** raises some interesting possibilities. The presence of two equally intense resonances as apparent triplets suggests that the dinuclear frameworks of **1** and **2** are retained. The existence of Hg–P coupling of similar magnitude on both sets suggests that the mercury(II) chloride interacts similarly with both the PIrP and PAuP portions. The magnitude of the coupling constants is too small for the presence of either Hg–P or *trans*-Hg–M–P units. The A-frame-like structures, **A** or **B** (where L is CO and Cl and n = 1 for **4** and L = $CNCH_3$ and n = 2 for **6**), are likely possibilities for these intermediates. These structures are related to that of **7**, the

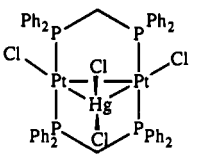

7

mercury(II) chloride adduct of $Pt_2(\mu\text{-}dpm)_2Cl_2$.[20] Notice that **1**, **2**, and $Pt_2(\mu\text{-}dpm)_2Cl_2$ are isoelectronic, 30-electron complexes. The d^8–d^{10} dimers **1** and **2** have an unsymmetrical 4:2 ligand arrangement with a long metal–metal separation, while the d^9–d^9 dimer has 3:3 ligand arrangement. The similarity in electron count for **1**, **2**, and $Pt_2(\mu\text{-}dpm)_2Cl_2$ suggests that the bonding with mercury(II) chloride may occur in a similar fashion. In **7**, two-bond P–Hg coupling is observed with $^2J(Hg,P)$ = 151.2 Hz. This value is of roughly the same magnitude as the corresponding values seen for intermediates **4** and **6**. The fact that the two Hg–P coupling constants are different in **4** and **6** might be interpreted to indicate that the mercury atom is asymmetrically disposed on the Ir–Au unit. However, there is no assurance that the Hg–Au–P and Hg–Ir–P paths of spin coupling will produce coupling constants of the same size for equivalently strong Hg–Au and Hg–Ir bonds. Consequently, it is inappropriate to infer that the mercury atom is necessarily asymmetrically bound to the Ir–Au unit in **4** and **6**.

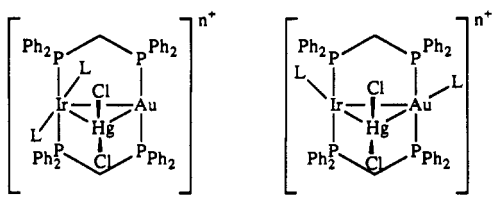

A **B**

Crystal and Molecular Structure of $Cl_2Hg(\mu\text{-}Cl)_2HgIr(CO)Cl(dpm)(\mu\text{-}dpmAuCl)\cdot 1.5CH_3OH$ (5). Compound **5** crystallizes with one complex molecule and 1.5 molecules of methanol within the asymmetric unit. The methanol molecules are not close enough to any of the metal ions to bond to them. A view of the complex is shown in Figure 4. Table I contains selected atomic coordinates. Table II gives a list of relevant bond distances and angles.

Compound **5** contains four metal ions each with different coordination numbers: 2, 3, 4, and 6. The iridium ion is six-coordinate with bonds to a chelating dpm ligand, trans carbon monoxide and chloride ligands, a mercury ion, and a bridging dpm ligand. The last is also bonded to a AuCl group. The P–Au–Cl group is linear as expected. Hg(1) is three-coordinate with bonds to iridium and the two bridging chlorides, while Hg(2) is four-coordinate with bonds to two bridging chlorides and two terminal chloride ligands.

The $Cl_2Hg(\mu\text{-}Cl)_2HgIr$ unit represents an unusual feature within this molecule. Generally, mercury(II) chloride reacts with

(18) $^2J(Hg,P)_{cis}$ is 397 Hz while $^2J(Hg,P)_{trans}$ is 3879 Hz in ClHgIrCl(PPh$_3$)$_2$(C(O)NRNNR): van Vliet, P. I.; Kuyper, J.; Vrieze, K. *J. Organomet. Chem.* **1976**, *122*, 99.

(19) Pregosin, P. S.; Kunz, R. W. *^{31}P and ^{13}C NMR of Transition Metal Phosphine Complexes*; Springer-Verlag: Berlin, 1979; p 121.

(20) Sharp, P. R. *Inorg. Chem.* **1986**, *25*, 4185.

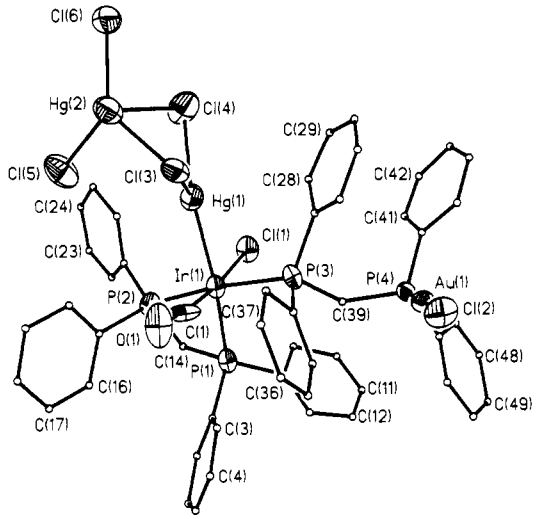

Figure 4. Perspective drawing of $Cl_2Hg(\mu\text{-}Cl)_2HgIr(CO)Cl(dpm)(\mu\text{-}dpmAuCl)$ using 50% thermal contours for anisotropically refined atoms and uniform, arbitrarily sized circles for carbon atoms of the dpm ligands.

Table I. Selected Atomic Coordinates ($\times 10^4$) and Equivalent Isotropic Displacement Coefficients ($Å^2 \times 10^3$) for $Cl_2Hg(\mu\text{-}Cl)_2HgIr(CO)Cl(dpm)(\mu\text{-}dpmAuCl)\cdot 1.5CH_3OH$

	x	*y*	*z*	*U*(eq)[a]
Ir(1)	2598 (1)	1922 (1)	3019 (1)	31 (1)
Au(1)	4969 (1)	255 (1)	1287 (1)	34 (1)
Hg(1)	1399 (1)	2453 (1)	2139 (1)	53 (1)
Hg(2)	966 (2)	3635 (1)	1250 (1)	63 (1)
P(1)	3359 (8)	1495 (3)	3947 (4)	39 (3)
P(2)	2015 (7)	2422 (3)	3907 (4)	35 (3)
P(3)	3210 (8)	1306 (3)	2236 (3)	34 (3)
P(4)	3400 (7)	84 (3)	1944 (3)	29 (3)
O(1)	4752 (24)	2659 (8)	2807 (11)	73 (11)
Cl(1)	651 (7)	1449 (3)	3163 (4)	44 (3)
Cl(2)	6568 (8)	434 (3)	619 (4)	53 (3)
Cl(3)	2849 (7)	2968 (3)	1119 (3)	47 (3)
Cl(4)	−430 (8)	2722 (3)	1486 (5)	74 (4)
Cl(5)	1160 (10)	3863 (4)	2322 (4)	79 (4)
Cl(6)	71 (9)	3910 (3)	302 (4)	72 (4)
C(1)	3991 (30)	2354 (14)	2899 (13)	47 (14)
C(14)	2289 (26)	1862 (9)	4441 (12)	36 (8)
C(39)	3136 (28)	617 (10)	2504 (13)	42 (8)

[a] Equivalent isotropic *U* defined as one-third of the trace of the orthogonalized U_{ij} tensor. Phenyl ring and methanol parameters are omitted; see supplementary material.

Ir(I) compounds by oxidative addition to create ClHgIrCl units.[18,21] The Hg–Ir distance (2.618 (3) Å) is just slightly longer than the corresponding distance (2.570 (1) Å) in $ClHgIrCl_3(CO)(PPh_3)_2$, where the mercury is only two-coordinate.[21] In **5**, Hg(1) is three-coordinate and nearly planar. The sum of the Cl–Hg–Cl and two Ir–Hg–Cl angles is 358.8°. However, the arrangement is otherwise far from regular. The Cl(3)–Hg–Cl(4) angle is only 82.9 (3)°, while the Ir–Hg–Cl(4) angle is 156.1 (2)° and the Ir–Hg–Cl(3) angle is 119.8 (2)°. Likewise the coordination about Hg(2) shows a high degree of angular variability. The narrowest Cl–Hg–Cl angle (84.3 (2)°) again involves the two bridging chloride ligands, while the widest (142.9 (3)°) involves the two terminal chloride ligands. The other Cl–Hg–Cl angles range from 93.5 (3) to 113.3 (3)°. There is also a wide variation in the Hg–Cl distances (2.330 (9)–2.985 (8)°). The short distances involve the two terminal chlorides Cl(5) and Cl(6), while the longest is the Hg(1)–Cl(3) distance. For comparison the Hg–Cl distances in $HgCl_2$ are 2.284 (12) and 2.301 (14) Å.[22] In $ClHgIrCl_3(CO)(PPh_3)_2$ the Hg–Cl distance is 2.366 (4) Å.[21]

Table II. Bond Lengths (Å) and Angles (deg) for $Cl_2Hg(\mu\text{-}Cl)_2HgIr(CO)Cl(dpm)(\mu\text{-}dpmAuCl)\cdot 1.5CH_3OH$

Bond Lengths			
Ir(1)–Hg(1)	2.618 (3)	Ir(1)–P(1)	2.385 (8)
Ir(1)–P(2)	2.369 (8)	Ir(1)–P(3)	2.381 (8)
Ir(1)–Cl(1)	2.405 (8)	Ir(1)–C(1)	1.85 (3)
Au(1)–P(4)	2.238 (8)	Au(1)–Cl(2)	2.282 (8)
Hg(1)–Cl(3)	2.985 (8)	Hg(1)–Cl(4)	2.463 (9)
Hg(2)–Cl(3)	2.623 (8)	Hg(2)–Cl(4)	2.779 (9)
Hg(2)–Cl(5)	2.370 (9)	Hg(2)–Cl(6)	2.330 (9)
Bond Angles			
Hg(1)–Ir(1)–P(1)	168.7 (2)	Hg(1)–Ir(1)–P(2)	100.2 (2)
P(1)–Ir(1)–P(2)	70.1 (3)	Hg(1)–Ir(1)–P(3)	87.7 (2)
P(1)–Ir(1)–P(3)	101.6 (3)	P(2)–Ir(1)–P(3)	171.1 (3)
Hg(1)–Ir(1)–Cl(1)	86.5 (2)	P(1)–Ir(1)–Cl(1)	87.1 (3)
P(2)–Ir(1)–Cl(1)	85.6 (3)	P(3)–Ir(1)–Cl(1)	90.8 (3)
Hg(1)–Ir(1)–C(1)	88.8 (10)	P(1)–Ir(1)–C(1)	96.9 (9)
P(2)–Ir(1)–C(1)	91.2 (10)	P(3)–Ir(1)–C(1)	93.2 (10)
Cl(1)–Ir(1)–C(1)	173.7 (11)	P(4)–Au(1)–Cl(2)	179.7 (5)
Ir(1)–Hg(1)–Cl(3)	119.8 (2)	Ir(1)–Hg(1)–Cl(4)	156.1 (2)
Cl(3)–Hg(1)–Cl(4)	82.9 (3)	Cl(3)–Hg(2)–Cl(4)	84.3 (2)
Cl(3)–Hg(2)–Cl(5)	101.8 (3)	Cl(4)–Hg(2)–Cl(5)	93.5 (3)
Cl(3)–Hg(2)–Cl(6)	113.3 (3)	Cl(4)–Hg(2)–Cl(6)	101.1 (3)
Cl(5)–Hg(2)–Cl(6)	142.9 (3)	Ir(1)–P(2)–C(14)	93.0 (8)
Hg(1)–Cl(3)–Hg(2)	78.2 (2)	Hg(1)–Cl(4)–Hg(2)	85.0 (3)
Ir(1)–C(1)–O(1)	173 (3)	P(1)–C(14)–P(2)	96.9 (13)
P(3)–C(39)–P(4)	118.8 (15)		

The ability of mercury(II) chloride to interact with terminal M–Cl bonds[23] and with itself has been noted earlier.[24] The work of Cabeza and co-workers, which has shown stepwise addition of two mercury(II) halides to $Ru_2(\mu\text{-naphthalene-1,8-diamine})(CO)_6$, is of particular relevance.[24] In that case in the adduct $Ru_2(\mu\text{-dan})(CO)_6Hg(\mu\text{-}Cl)_2HgCl_2$, a planar, four-coordinate mercury(II) is present, while **5** contains a planar, three-coordinate mercury (along with four-coordinate, pseudotetrahedral mercury(II) in both cases).

The formation of **5** involves at least opening of the $Au(\mu\text{-dpm})_2Ir$ unit at one P–Au bond and readdition of that phosphorus to the iridium to form the chelate ring. The gold ion acquires a chloride ligand (possibly from mercury(II) chloride), and two mercury(II) chloride units are attached to the iridium, which has coordination geometry characteristic of Ir(III). The degree of rearrangement involved in the formation of **5** is interesting since many dpm-bridged dinuclear complexes undergo chemical reactions that leave the dinuclear framework intact.

Experimental Section

Preparation of Compounds. Complexes **1**[25] and **2**[6] were prepared as described previously.

$Cl_2Hg(\mu\text{-}Cl)_2HgIr(CO)Cl(dpm)(\mu\text{-dpmAuCl})$. Mercury(II) chloride (26 mg, 0.098 mmol) was added to a stirred solution of 67 mg (0.049 mmol) of **1** dissolved in 25 mL of acetone. After 30 min the orange solution had turned yellow. The solution was filtered, and the solvent volume was reduced to 4 mL. Addition of ethyl ether produced a pale yellow solid, which was collected by filtration and washed with ethyl ether (yield 70%). Infrared (Nujol mull): ν(CO), 2060 cm^{-1}. $^{31}P\{^1H\}$ NMR (dichloromethane): δ = 18.3 ppm (P(4)); δ_2 = −24.3 ppm (J(P,P) = 325 Hz), J(Hg,P) = 225 Hz; P(3)); δ_3 = −46.2 ppm (J(P,P) = 325 Hz, P(2)); δ_4 = −56.3 ppm (J(Hg,P) = 3822 Hz; P(1)). Crystals suitable for X-ray crystallography were obtained by diffusion of methanol into a dichloromethane solution of the complex.

Reaction of $[AuIr(CO)Cl(\mu\text{-dpm})_2](PF_6)$ (1) with Boron Trifluoride. A 5 mM solution of **1** in dichloromethane was prepared. The $^{31}P\{^1H\}$ NMR spectrum obtained from this orange solution consisted of a pair of pseudotriplets δ_1 = 18.6 ppm and δ_2 = 31.0 ppm (N = 56 Hz) for the cation.[23] Passage of a stream of boron trifluoride vapor through this solution for 30 s resulted in a color change to light yellow. The $^{31}P\{^1H\}$ NMR spectrum exhibited a pair of resonances at δ_1 = 20.0 ppm and δ_2 = 38.0 ppm (N = 54.7 Hz) for the cation. The resonances of **1** were no

(21) Brotherton, P. D.; Raston, C. L.; White, A. H.; Wild, S. B. *J. Chem. Soc., Dalton Trans.* **1976**, 1799.
(22) Subramanian, V.; Seff, K. *Acta Crystallorg.*, Sect. B **1980**, *B36*, 2132.
(23) Barr, R. M.; Goldstein, M.; Hairs, T. N. D.; McPartlin, M.; Markwell, A. J. *J. Chem. Soc., Chem. Commun.* **1974**, 221.
(24) Cabeza, J. A.; Fernández-Colinas, J. M.; Garcia-Granda, S.; Riera, V.; Van der Maelen, J. F. *J. Chem. Soc., Chem. Commun.* **1991**, 168.
(25) Hutton, A. T.; Pringle, P. G.; Shaw, B. L. *Organometallics* **1983**, *2*, 1889.

Table III. Crystallographic Data for $Cl_2Hg(\mu\text{-}Cl)_2HgIr(CO)Cl(dpm)(\mu\text{-}dpmAuCl)\cdot 1.5CH_3OH$

$C_{52.5}H_{44}AuCl_6Hg_2IrO_{2.5}P_4$	fw = 1841.8
a = 10.594 (7) Å	$P2_1/c$ (No. 14), monoclinic
b = 25.12 (2) Å	T = 130 K
c = 21.397 (13) Å	λ(Mo Kα) = 0.71073 Å
β = 91.04 (5)°	μ(Mo Kα) = 106.9 cm^{-1}
V = 5698 (7) Å^3	d_{calcd} = 2.147 Mg·m^{-3}
Z = 4	transm factors = 0.52–0.70
$R(F_o)^a$ = 0.066	$R_w(F_o)^a$ = 0.061

$^a R = \sum||F_o| - |F_c||/|F_o|$; $R_w = \sum||F_o| - |F_c||w^{1/2}/\sum|F_o w^{1/2}|$; $w^{-1} = \sigma^2|F| = 0.0003F^2$.

longer present. This solution was stable for at least 2 h when excess boron trifluoride was present. When the solvent was evaporated or when diethyl ether was added to precipitate the complex, the color of the sample returned to orange and only unreacted **1** was recovered. When a similar experiment was conducted with **2**, the $^{31}P\{^1H\}$ NMR spectrum of the colorless solution showed loss of resonances of **2** and appearance of 10 singlets between 40 and -65 ppm. Attempts to recover **2** from this mixture were unsuccessful.

Observation of Intermediates in the Reaction of 1 and 2 with Mercury(II) Chloride. A solution of **1** (5 mM) in dichloromethane was prepared in a 5-mm NMR tube. The sample was cooled to −78 °C in an acetone/dry ice bath. Three equivalents of solid mercury(II) chloride were added to the cold sample, which was vigorously shaken. This solution was transferred to the previously cooled probe of the NMR spectrometer, and the data in Figure 1 were collected. Attempts to isolate the adduct by crystallization through diffusion of either to the sample at −78 °C were unsuccessful. Similarly, a 5 mM acetone solution of **2** was prepared and cooled to −78 °C. Addition of solid mercury(II) chloride gave the sample which was used to obtain the data shown in Figure 3. This sample was stable to warming to 10 °C. At 23 °C the resonances of the intermediate were lost and new resonances of a species similar to **5** developed (δ_1 = 18 ppm, δ_2 = 17 ppm (J(P,P) = 289 Hz), δ_3 = −47 ppm (J(P,P) = 280 Hz), δ_4 = −61 ppm) along with singlets at 19, −22, −25, and −48 ppm. The signal to noise ratio did not allow mercury satellites to be observed.

X-ray Data Collection. Ivory parallelepipeds of the complex were coated with a light hydrocarbon oil, mounted on a glass fiber with silicon grease, and placed in the 130 K nitrogen stream of a Siemens R3m/V diffractometer that was equipped with a locally modified low-temperature apparatus. Unit cell parameters were determined by least-squares refinement of 28 reflections with $10° < 2\theta < 21°$. The unique space group $P2_1/c$ (No. 14) was determined by the following conditions: $0k0$, $k = 2n$; $h0l$, $l = 2n$. Two check reflections showed only random (<2%) fluctuation in intensity during data collection. The data were corrected for Lorentz and polarization effects. Crystal data are given in Table III. Scattering factors and corrections for anomalous dispersion were taken from a standard source.[26]

Solution and Structure Refinement. Calculation were performed using the Siemens SHELXTL PLUS system of programs. The structure was solved by direct methods. The carbon atoms of the dpm ligands and the carbon and oxygen atoms of methanol were refined isotropically, while all other atoms were refined anisotropically. Hydrogen atoms were included in the refinement model. Their positions were calculated by the use of a riding mode with C–H distance fixed at 0.96 Å and a thermal parameter of U = 0.05 Å.[2] An absorption correction was applied.[17]

Acknowledgment. We thank the National Science Foundation (Grant CHE 9022909) for support and Johnson-Matthey, Inc., for a loan of precious metal salts.

Supplementary Material Available: Tables of crystal data, atomic positional parameters, bond distances, bond angles, anisotropic thermal parameters, and hydrogen atom positions for **5** (10 pages); a listing of structure factors for **5** (27 pages). Ordering information is given on any current masthead page.

(26) *International Tables for X-ray Crystallography*; Kynoch Press: Birmingham, England, 1974; Vol. 4.
(27) The method obtains an empirical absorption tensor from an expression relating F_o and F_c: Moezzi, B. Ph.D. Thesis, University of California, Davis, 1987.

Contribution from the Department of Chemistry,
The Pennsylvania State University, University Park, Pennsylvania 16802

Synthesis and Structure of Small-Molecule Cyclic Phosphazenes Bearing Ortho-Substituted Aryloxy and Phenoxy Substituents

Harry R. Allcock,* Alexa A. Dembek, Michael N. Mang, Geoffrey H. Riding, Masood Parvez, and Karyn B. Visscher

Received February 21, 1992

A series of cyclic trimeric and tetrameric phosphazenes with ortho-substituted aryloxy side groups have been synthesized. The ortho substituents are methyl and phenyl groups. These compounds are structural models for the corresponding linear high-polymeric phosphazenes. X-ray structural analysis of the cyclic tetrameric species $[NP(OC_6H_4CH_3\text{-}2)_2]_4$ (**3**), $[NP(OC_6H_4C_6H_5\text{-}2)_2]_4$ (**4**), and $[NP(OC_6H_5)_2]_4$ (**5**) are reported. Crystals of **3** are triclinic with space group $P\bar{1}$, with a = 11.494 (3) Å, b = 12.348 (2) Å, c = 30.181 (5) Å, α = 80.88 (1)°, β = 88.19 (2)°, γ = 71.23 (1)°, V = 4003.6 Å^3, and Z = 3. Crystals of **4** are orthorhombic with space group $Pna2_1$, with a = 25.177 (2) Å, b = 20.472 (3) Å, c = 17.256 (3) Å, V = 8894.1 Å^3, and Z = 4. Finally, crystals of **5** are triclinic with space group $P\bar{1}$, with a = 11.514 (2) Å, b = 11.567 (2) Å, c = 17.761 (1) Å, α = 79.21 (1)°, β = 79.87 (1)°, γ = 81.21 (1)°, V = 2269.8 Å^3, and Z = 2.

High-polymeric phosphazenes comprise a broad class of inorganic/organic hybrid macromolecules with the general formula $[NPR_2]_n$ (where n = 15000). The specific physical or chemical properties of these polymers are imposed by the structure of the organic, inorganic, or organometallic side group.[1,2] For example, different side groups generate properties such as liquid-crystallinity,[3] nonlinear optical character,[4] or utility as biomedical materials.[5]

In an earlier paper, we reported the synthesis of a series of poly((aryloxy)phosphazenes) with phenylphenoxy and related

(1) (a) Allcock, H. R.; Kugel, R. L. *J. Am. Chem. Soc.* **1965**, *87*, 4216. (b) Allcock, H. R.; Kugel, R. L.; Valan, K. J. *Inorg. Chem.* **1966**, *5*, 1709. (c) Allcock, H. R.; Kugel, R. L. *Inorg. Chem.* **1966**, *5*, 1716. (d) Allcock, H. R. *Chem. Eng. News* **1985**, *63*, 22.
(2) (a) Allcock, H. R.; Allen, R. W.; Meister, J. J. *Macromolecules* **1976**, *9*, 950. (b) Allen, R. W.; Allcock, H. R. *Macromolecules* **1976**, *9*, 956.
(3) (a) Allcock, H. R.; Kim, C. *Macromolecules* **1989**, *22*, 2596. (b) Allcock, H. R.; Kim, C. *Macromolecules* **1990**, *23*, 3881.
(4) Allcock, H. R.; Dembek, A. A.; Kim, C.; Devine, R. L. S.; Shi, Y.; Steier, W. H.; Spangler, C. W. *Macromolecules* **1991**, *24*, 1000.
(5) (a) Laurencin, C. T.; Koh, H. J.; Neenan, T. X.; Allcock, H. R.; Langer, R. *J. Biomed. Mater. Res.* **1987**, *21*, 1231. (b) Cohen, S.; Bano, M. C.; Visscher, K. B.; Chow, M.; Allcock, H. R.; Langer, R. *J. Am. Chem. Soc.* **1990**, *112*, 7832.

0020-1669/92/1331-2734$03.00/0